Communication

Alkylated Trimethylene-Bridged Bis(*p*-Phenylenediamines)

Stephen F. Nelsen, Gaoquan Li, Kevin P. Schultz, Hieu Q. Tran, Ilia A. Guzei, and Dennis H. Evans

J. Am. Chem. Soc., **2008**, 130 (35), 11620-11622 • DOI: 10.1021/ja802292g • Publication Date (Web): 12 August 2008

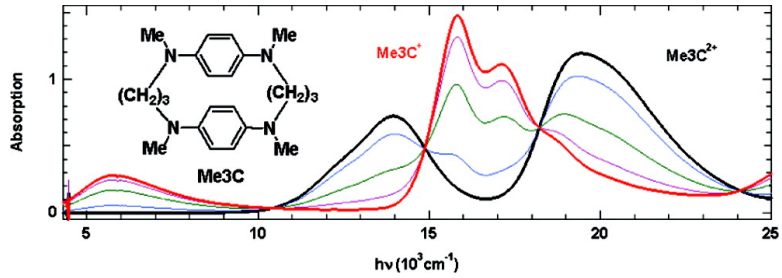

More About This Article

Additional resources and features associated with this article are available within the HTML version:

- Supporting Information
- Access to high resolution figures
- Links to articles and content related to this article
- Copyright permission to reproduce figures and/or text from this article

View the Full Text HTML

J|A|C|S
COMMUNICATIONS

Published on Web 08/12/2008

Alkylated Trimethylene-Bridged Bis(*p*-Phenylenediamines)

Stephen F. Nelsen,* Gaoquan Li, Kevin P. Schultz, Hieu Q. Tran, and Ilia A. Guzei†

Department of Chemistry, University of Wisconsin, 1101 University Avenue, Madison, Wisconsin 53706-1396 and Molecular Structure Laboratory, Chemistry Department, University of Wisconsin, 1101 University Avenue, Madison, Wisconsin 53706-1396

Dennis H. Evans

Department of Chemistry, University of Arizona, 1306 East University, Tucson, Arizona 85721

Received April 2, 2008; E-mail: nelsen@chem.wisc.edu

There is great interest in radical ion systems that interact in face-to-face "π-stacking" geometries, as exemplified by the large literature on electron transfer down DNA stacks[1] as well as on oxidized hexaarylbenzene derivatives,[2] and stacked methylene-bridged fluorene radical ions.[3] At the beginning of matrix studies on unstable aromatic hydrocarbon radical cations, Brockelhurst discovered that long wavelength absorptions that he called *charge resonance* bands are caused by dimeric radical cations.[4] Kosower showed that even the quite stable charged π system methylviologen radical cation ($MV^{\bullet+}$) dimerizes to form a singlet species with

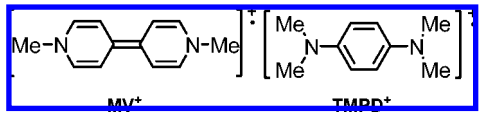

characteristic changes in its optical absorption spectrum, named the process pimerization, and predicted that it would occur generally for radicals and radical ions.[5] Considerable work on intermolecular MV^{+} dimers,[6] singly and doubly bridged intramolecular dimeric viologen derivatives,[7] and dendrimeric versions with up to 45 viologen units[8] has established the generality of pimerization for viologen radical cations and determined the temperature dependence of the equilibrium constant. Grampp and co-workers studied the pimerization equilibria for a variety of intermolecular radical cation, neutral, and radical anion examples by ESR, including *p*-phenylene diamine radical cation (**PD**$^{\bullet+}$) examples such as **TMPD**$^{\bullet+}$ that are monomeric versions of the compounds studied here.[9] Kochi and co-workers have extended this work to obtaining X-ray structures for radical ion dimers, including both the diamagnetic radical cation dimer (**OMB**$^{\bullet+}$)$_2^{2+}$ and the paramagnetic radical cation, neutral dimer, (**OMB**)$_2^{\bullet+}$,[10] and have also studied the temperature effect on forming both types of dimers of cation, neutral, and anion radicals.[10] Goodson, Hartwig, and co-workers studied optical spectra

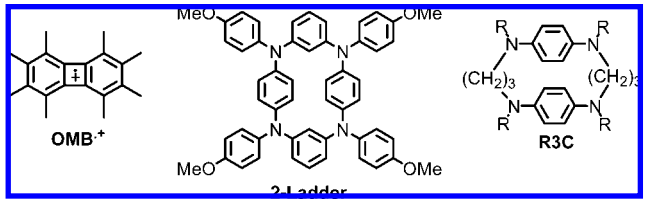

of the tetra-*p*-anisyl-tetraazacyclophane **2-Ladder** and three and four **PD** unit-containing analogues.[11] This work focuses on dimeric paracyclophanes that have $(CH_2)_n$ bridges with $n = 3$ that doubly link the nitrogens of two **PD** units and have the same alkyl substituent occupying the other four positions for substitution at

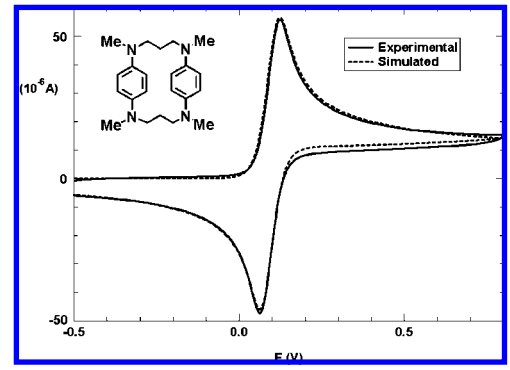

Figure 1. Simulation of the region for removal of the first two electrons from a 0.9 mM solution of **Me3C** in MeCN containing 0.1 M Bu_4NClO_4, scan rate 100 mV/s. Simulation parameters: $E°_1 = 0.102$ V, $E°_2 = 0.082$ V, $D = 1.85 \times 10^{-5}$ cm^2/s, solution resistance = 160 ohms, electrode area = 0.071 cm^2. reference electrode aq. SCE.

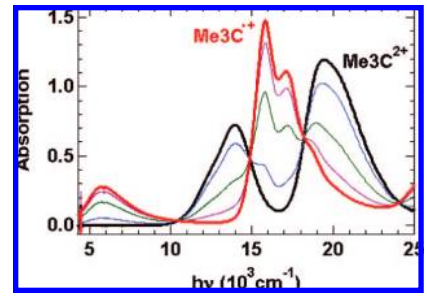

Figure 2. Titration of a CH_2Cl_2 solution of **Me3C**$^{2+}(PF_6)_2$ (black) with increments of a solution of neutral **Me3C** to convert it to a mixture rich in **Me3C**$^{\bullet+}$ (red).

nitrogen, which we abbreviate **RnC**. This paper reports on oxidized **Me3C**, **Et3C**, and **iPr3C**, which have been studied as both radical cations and diradical dications. Oxidation of **Me3C** and **Me5C** was studied earlier by Takemura and co-workers.[12] They concluded that **Me3C**$^{+}$ could not be obtained and found that **Me3C**$^{2+}$ is diamagnetic but **Me5C**$^{2+}$ is paramagnetic. As pointed out earlier, the first two oxidation waves of **Me3C** in MeCN overlap.[12] The simulation of the cyclic voltammogram in acetonitrile shown in Figure 1 gave a slightly negative value of $(E_2° - E_1°)$, −20 mV. The dication is converted to the monocation by addition of a neutral compound, as shown in Figure 2 for data taken in methylene chloride. The four isosbestic points are consistent with a simple equilibrium between two stable species that absorb light in this region. Fitting the intermediate spectra as sums of weighted spectra of (•+) and (2+) to give concentrations of (•+) and (2+) gave values which when fit to the comproportionation equilibrium of eq 1 gave K_{comp} values in acetonitrile of ∼3.3, 2.50, 2.46, and 2.48 as

† Molecular Structure Laboratory.

10.1021/ja802292g CCC: $40.75

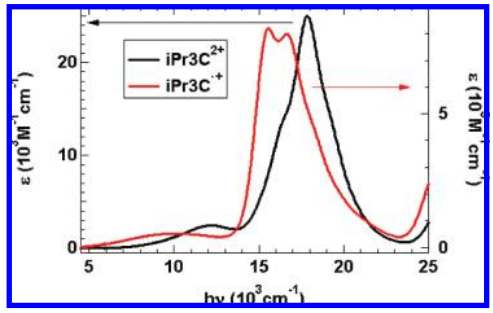

Figure 3. Comparison of **iPr3C**$^{\bullet+}$ (red) and **iPr3C**$^{2+}$ (black) spectra in CH_2Cl_2.

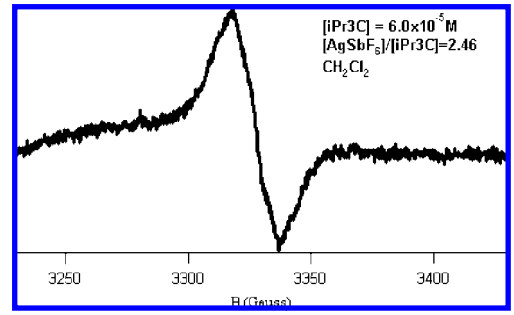

Figure 4. ESR spectrum of **iPr3C**$^{2+}$ in methylene chloride solution at room temperature.

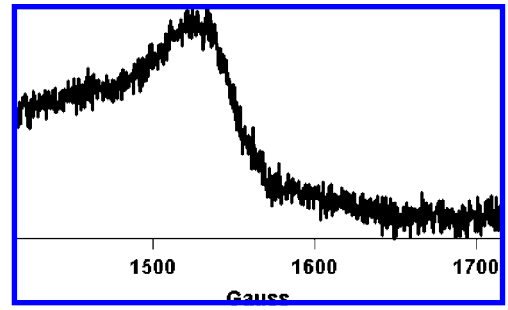

Figure 5. Half-field region of the ESR spectrum of **iPr3C**$^{2+}$ in a 1:1:1 MeCN/PrCN/CH_2Cl_2 glass at 120 K.

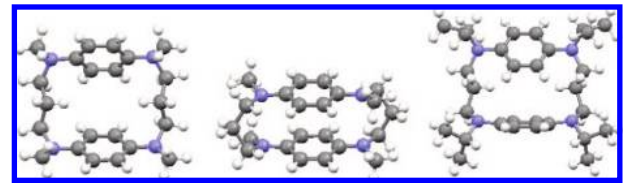

Figure 6. X-ray structures of (left) **Me3C**^{0}, (middle) **Me3C**$^{2+}$ (anti diastereomer fragment of $(PF_6^-)_2$ 2MeCN salt), (right) **iPr3C**^{0}.

more neutral compound is added, corresponding to ($E_2°$ - $E_1°$) values of +30, 23.5, 23.1 and 23.3 mV.[13]

$$K_{comp} = [\bullet +]^2/([2+][0]) \quad (1)$$

We conclude that the first two oxidation potentials are very close to each other, which needs rationalization for a compound having two **PD**$^{+}$ rings held so close together. **Et3C** has a similar cyclic voltammogram to that of **Me3C**, also with overlapping waves for first and second electron removal, but **iPr3C** has these waves well separated, by 0.29 V. The X-ray structures reported below suggest why the large difference in $E°$ values occurs.

The region near 16 000 cm^{-1} in the spectrum of **Me3C**$^{\bullet+}$ is clearly the highest doubly occupied to singly occupied molecular orbital (HOMO to SOMO) vertical excitation within a single oxidized **PD**$^{\bullet+}$ unit.[15] Its maximum at 15 820 cm^{-1} in CH_2Cl_2 occurs 410 cm^{-1} lower in energy than that of the "monomeric" **TMPD**$^{\bullet+}$ in CH_2Cl_2,[16] and two vibrational structure features are resolved as maxima in each, although the first feature is in a 1.2 ε_{max} ratio to the second for **Me3C**$^{\bullet+}$ and a 1.0 ratio for **TMPD**$^{\bullet+}$. We assign the very broadband at ~5800 cm^{-1} in Figure 2 as a Hush-type[17] Class II (localized)[18] mixed valence charge transfer band corresponding to electron transfer from **PD**^{0} to **PD**$^{\bullet+}$. In contrast, **Me$_3$C**$^{2+}$ shows no mixed valence band and broadened absorptions that show no resolved vibrational fine structure at 14 000 and 19 500 cm^{-1} (ε ratio 1.8), as if there were an ~5500 cm^{-1} splitting between two **PD**$^{\bullet+}$ HOMO to SOMO excitations. **Et3C** shows similar behavior to that of **Me3C**, but **iPr3C** cations and dications have optical properties that are quite different from those of their unbranched alkyl analogues (see Figure 3). **iPr^{3}C**$^{\bullet+}$ has its HOMO to SOMO vertical **PD**$^{\bullet+}$ excitation at 15 500 cm^{-1}, 320 cm^{-1} lower energy than that of its methyl analogue and is somewhat broader, while its mixed valence band occurs at 10 000 cm^{-1}, 4200 cm^{-1} higher in energy. **iPr3C**$^{2+}$ shows unresolved bands at 12 200 and 17 800 cm^{-1} (ε ratio 10). The relationship of these absorptions to those of **Me3C**$^{2+}$ is not at all clear to us.

It is well established that trimethylene bridges between π systems such as those of **V**$^{+}$ allow association and produce singlet species, but although **Me3C**$^{2+}$ and **Et3C**$^{2+}$ exhibit only weak and broad ESR signals at room temperature, **iPr3C**$^{2+}$ (as well as **iPr4C**$^{2+}$, **Me5C**$^{2+}$, and **iPr5C**$^{2+}$, to be documented in a future publication) exhibits a much stronger ESR signal in solution (see Figure 4), indicating that **iPr3C**$^{2+}$ has a significantly smaller singlet, triplet gap than does **Me3C**$^{2+}$. At 120 K in a 1:1:1 acetonitrile/butyronitrile/methylene chloride glass triplet features are observed near $g = 2$ for **iPr3C**$^{2+}$, as well as a "half-field" $\Delta M_s = 2$ transition that is characteristic of triplets (see Figure 5).

X-ray crystallographic studies suggest why **Me3C** and **iPr3C** show such different behavior upon oxidation. Ball and stick representations of the X-ray crystallographic structures of **Me3C**^{0}, **Me3C**$^{2+}$, and **iPr3C**^{0} are shown in Figure 6. These structures seem most naturally grouped using the twist angles at the NCCC and CCCN′ bonds of their $(CH_2)_3$ bridging units which can be any combination of *gauche* and *anti* (*g* and *a*); see below for diagramatic representation of *aa* and gg conformations. **Me3C**^{0} crystallizes in the double *aa* conformation

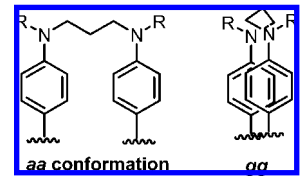

that keeps the rings as far apart as they can be, but removal of two electrons results in attractive interactions between the **PD**$^{+}$ units that cause the conformation to change, and the diradical dication **Me3C**$^{2+}$ crystallizes in the double *gg* conformation that holds the **PD** rings nearly parallel (the angle between the aryl rings is labeled Ar∠ in the Table 1) and much closer together, significantly less than the 3.1 Å sum of van der Waals radii at nitrogen and 3.4 Å at carbon for the anti conformation. Both *anti* (C_i symmetry) (as indicated in the diagram above) and *syn* methyl double *gg* conformations were present in the disordered **Me3C**$^{2+}$ crystals.

The NMR spectrum of an MeCN solution of **Me3C**$^{2+}$ was very broadened at room temperature, but it sharpens considerably upon lowering the temperature (see Figure 7). Because the triplet would have an extremely broad NMR spectrum, Figure 7 shows that

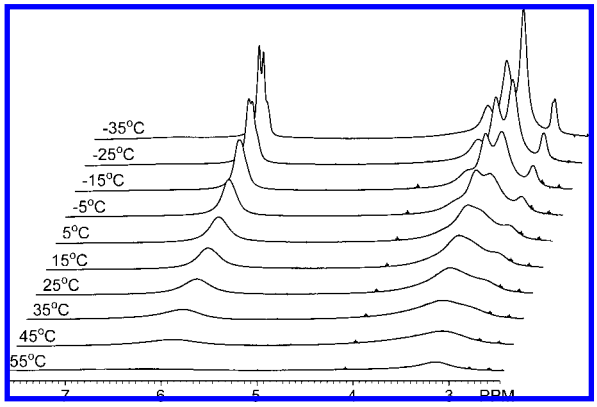

Figure 7. Stacked plots of ^{1}H-NMR spectra of **Me3C^{2+}** in acetonitrile-d_3 at the temperatures shown at the left.

Table 1. Parameters from the X-ray Structures of Figure 6

cmpd	Me3C^0	Me3C^{2+}	iPr3C^0
type	*aa*,*aa*	*gg*,*gg*	*ag*,*ag*
$d_{N,N'}$, Å	4.97, 4.98	2.94	4.33, 4.33
$d_{C,C}$, Å [a]	3.65, 3.67	3.084	3.75, 3.76
Ar∠, deg	68	0	49

[a] Smallest nonbonded aryl C,C distances for the high Ar∠ diastereomers, and 3.09 (C attached to N), 3.19, and 3.16 Å for **Me3C^{2+}**.

Me3C^{2+} has a singlet ground state with a thermally accessible triplet. Rotation of the aromatic rings on the NMR time scale would not occur because the rings are pressed so closely together, so each conformation present would be expected to show two singlets in the aromatic region. Unfortunately the signals are still too broad to tell conclusively whether *syn* and *anti* conformations are both present in solution as they were in the crystal, but it seems reasonable. The spectrum in acetone-d_6 shows approximately the same broadening at −65 °C as the acetonitrile-d_3 spectrum does at −25 °C, so our attempt to use a lower melting solvent to sharpen the spectrum failed because the triplet content is very sensitive to solvent. Single temperature Evans solvent shift magnetic susceptibility measurements[19] similar to those discussed by Blackstock and co-workers,[20] but including diamagnetic corrections,[21] give a triplet content of ∼1% for **Me3C^{2+}** and 34% for **iPr3C^{2+}** at room temperature in acetonitrile-d_3. Variable temperature experiments show complex behavior that is under study.

In contrast, the larger isopropyl groups of **iPr3C^0** cause it to crystallize as a double *ga* diastereomer. It is known that B3LYP calculations do not handle π-stacking interactions very well,[22] but each of these species is calculated using B3LYP/6-31G* to be most stable in the conformation in which it crystallized (although **Me3C^{2+}** is calculated to be more stable in the *syn* than in the *anti* conformation that predominated in the crystal). These calculations incorrectly predict triplet **Me3C^{2+}** to be more stable than the singlet and result in the nonbonded atom distances being larger than those of the X-ray structure (see Supporting Information for details).[23] We suggest that **iPr3C^{2+}** has a significantly higher triplet content than **Me3C^{2+}** and a very different optical spectrum because its *gg*,*gg* conformation is too high in energy to be populated.

The most surprising aspect of this work to us is the conformational sensitivity of these **PD**-based diradical dications to spin pairing, because intramolecular dimer radical cations of viologen radical cations with both single and double three- and four-carbon bridges are singlets.[6−8] The disappearance of the ESR spectrum has been used for years as the criterion for dimerization of π-delocalized radicals, including **PD$^{\bullet+}$**.[5−10] It appears that even though considerable splaying of the aryl rings that is present for hexaarylbenzene radical cations obviously allows large electronic interactions,[2] the **PD$^{\bullet+}$** ring is not flexible enough to allow close enough approach of the π systems for large enough π-stacking interactions to allow *gg*,*gg* conformations to predominate except in rather geometrically favorable circumstances.

Acknowledgment. We thank the NSF for support of this work under CHE-0204197 and -0647719, and John F. Berry for helpful instruction on Evans solvent shift measurements.

Supporting Information Available: Structural data reports, compound preparation, comparison of calculated with X-ray geometries and energies, coordinates for B3LYP/6-31G* optimized structures.The X-ray data are available free of charge from the Cambridge Structural Database as **Me3C^0** (CCDC 680468), **iPr3C^0** (CCDC 680469), **Me3C^{2+}**(PF$_6^-$)$_2$ 2MeCN (CCDC 680470). This material is available free of charge via the Internet at http://pubs.acs.org.

References

(1) (a) Wagenknecht, H.-A. *Charge transfer in DNA: From Mechanism to Application*; Wiley-VCH: Munich, 2005. (b) Lewis, F. D. In *Electron transfer and charge transport process in DNA*; Balzani, V., Gray, H. B., Winkler, J. R., Eds.; Electron Transfer in Chemistry; Wiley-VCH: Weinheim, 2001; Vol. 3, Part 1, Chapter 3, pp 105−176..
(2) (a) Lambert, C.; Nöll, G. *Angew. Chem., Int. Ed.* **1998**, *37*, 2107–2110. (b) Lambert, C.; Nöll, G. *Chem.—Eur. J.* **2002**, *8*, 3436. (c) Rathore, R.; Burns, C. L.; Deseinicu, M. I. *Org. Lett.* **2001**, *3*, 2887–2890. (d) Rathore, R.; Burns, C. L.; Abdelwahed, S. A. *Org. Lett.* **2004**, *6*, 1689–1692. (e) Chebny, V. J.; Shukla, R.; Rathore, R. *J. Phys. Chem. B* **2006**, *110*, 13003–13006. (f) Chebny, V. J.; Dhar, D.; Lindeman, S. V.; Rathore, R. *Org. Lett.* **2006**, *71*, 6124–6129. (g) Sun, D.; Rosokha, S. V.; Kochi, J. K. *Angew. Chem., Int. Ed.* **2005**, *44*, 5133–5136. (h) Rosokha, S. V.; Neretin, I. S.; Sun, D.; Kochi, J. K. *J. Am. Chem. Soc.* **2006**, *128*, 9394–9407.
(3) (a) Stevenson, D. D.; Kiesewetter, M. K.; Reiter, R. C.; Abdelwahed, S. H.; Rathore, R. *J. Am. Chem. Soc.* **2005**, *127*, 5282–5283. (b) Rathore, R.; Abdelwahed, S. H.; Kiesewetter, M. K.; Reiter, R. C.; Stevenson, C. D. *J. Phys. Chem. B* **2006**, *110*, 2536–1540.
(4) (a) Badger, B.; Brocklehurst, B. *Nature* **1968**, *219*, 263. (b) Badger, B.; Brocklehurst, B. *Trans. Faraday Soc.* **1969**, *65*, 2576, 2582, 2588.
(5) (a) Kosower, E. M.; Cotter, J. L. *J. Am. Chem. Soc.* **1964**, *86*, 5524–7. (b) Kosower, E. M.; Hajdu, J. *J. Am. Chem. Soc.* **1971**, *93*, 2534–5.
(6) (a) Evans, A. G.; Evans, J. C.; Rees, N. H. *J. Chem. Soc., Perkin Trans. 2* **1975**, 1831. (b) Evans, A. G.; Evans, J. C.; Baker, M. W. *J. Chem. Soc., Perkin Trans. 2* **1977**, 1787.
(7) Geuder, W.; Hünig, S.; Suchy, A. *Tetrahedron* **1986**, *42*, 1665–1677.
(8) Heinen, S.; Walder, L. *Angew. Chem., Int. Ed.* **2000**, *39*, 806–809.
(9) Grampp, G.; Landgraf, S.; Rasmussen, K.; Strauss, S. *Spectrochim. Acta A* **2002**, *58*, 1219–1226.
(10) (a) Kochi, J. K.; Rathore, R.; Le Magueres, P. *J. Org. Chem.* **2000**, *65*, 6826–6836. (b) Lü, J.-M.; Rosokha, S. V.; Kochi, J. K. *J. Am. Chem. Soc.* **2003**, *125*, 12161–12171.
(11) Yan, X. Z.; Pawlas, J.; Goodson, T., III; Hartwig, J. F. *J. Am. Chem. Soc.* **2005**, *127*, 9105–9116.
(12) Takemura, H.; Takehara, K.; Ata, M. *Eur. J. Org. Chem.* **2004**, *493*, 6–4941.
(13) The neutral compound does not absorb at all in the visible and near-IR region shown (25 000 cm^{-1} = 400 nm).
(14) The initial value corresponds to only 13% of neutral present, causing significantly larger error than later points in the titration, which correspond to 31, 49, and 60% neutral present. Similar data in MC were not analyzed well using eq 1 because $\Delta E°$ is significantly larger, causing much larger errors in K_{comp}, leading to considerable scatter and even negative (0) concentrations.
(15) Nelsen, S. F.; Weaver, M. N.; Telo, J. P.; Lucht, B. L.; Barlow, S. *J. Org. Chem.* **2005**, *70*, 9326–9333.
(16) Nelsen, S. F.; Tran, H. Q. *J. Phys. Chem. A* **1999**, *103*, 8139–8144.
(17) For reviews see: (a) Hush, N. S. *Prog. Inorg. Chem.* **1967**, *8*, 391–444. (b) Hush, N. S. *Coord. Chem. Rev.* **1985**, *64*, 135–157. (c) Marcus, R. A.; Sutin, N. *Biochim. Biophys. Acta* **1985**, *811*, 265–322. (d) Sutin, N. *Prog. Inorg. Chem.* **1983**, *30*, 441–499.
(18) Robin, M.; Day, P. *Adv. Inorg. Radiochem.* **1967**, *10*, 247–422.
(19) (a) Evans, D. F. *J. Chem. Soc.* **1959**, 2003–2005. (b) Live, D. H.; Chan, S. I. *Anal. Chem.* **1970**, *42*, 791–792.
(20) Stickley, K. R.; Selby, T. D.; Blackstock, S. C. *J. Org. Chem.* **1997**, *62*, 448–449.
(21) Bain, G. A.; Berry, J. F. *J. Chem. Ed.* **2008**, *85*, 532–536.
(22) Zhao, Y.; Truhlar, D. G. *Acc. Chem. Res.* **2008**, *41*, 157–167.
(23) (a) B3LYP/6-31G* calculations were carried out starting with the x-ray structures and with structures found by using Spartan '02[20b] to find 50−100 molecular mechanics conformations, followed by their geometry optimization at the proper oxidation level using AM1, and selecting a few for B3LYP optimization, with either Spartan or Gaussian03.[20c] (b) Spartan '02, Wavefunction Inc., Irvine, CA. . (c) Frisch, M. J. et. al. *Gaussian 03*, revision B05; Gaussian Inc.: Pittsburgh, PA, 2003.

JA802292G